NBUJPS
NBU Journal of Plant Sciences

ISSN No. 0974-6927
Vol. 17 (2025), pp. 41-51

Research Article

Antiproliferative and pro-apoptotic activities of *Caesalpinia sappan* L. heartwood extract against glioblastoma cells: an *in vitro* study

Rafia Shekh[a], Vikrant[b], Rohit Kumar Tiwari[c], Sameen Shafi[d], Preeti Bajpai[d], Shahana Majumder[e]*

[a]Department of Biosciences, Integral University, Lucknow, Uttar Pradesh, India
[b]Department of Botany, School of Basic and Applied Sciences, Sanskaram University, Jhajjar, Haryana, India
[c]Department of Clinical Research, Sharda School of Allied Health Sciences, Sharda University, Gautam Budh Nagar, Uttar Pradesh, India
[d]Department of Zoology, Mahatma Gandhi Central University, Motihari, East-Champaran, Bihar, India
[e]Department of Botany, Mahatma Gandhi Central University, Motihari, East-Champaran, Bihar, India

Abstract

Glioblastoma multiforme (GBM) remains a formidable oncological challenge in the realm of brain diseases. The inherent limitations of contemporary GBM treatment options have spurred scientific exploration of natural compounds as potential alternatives or adjunct therapies. In this study, we present findings that shed light on the presence of various bioactive constituents in Caesalpinia sappan heartwood (CsHw-EtOH) identified by GC-MS analysis. Further, the anticancer potential of CsHw-EtOH was evaluated against GBM. *In vitro* studies demonstrated a significant reduction in the viability of rat glioblastoma C6 cells, accompanied by marked morphological alterations, particularly at an extract concentration of 60 µg/mL ($p < 0.01$). DCFH-DA-based analysis revealed a dose-dependent increase in intracellular ROS levels, with a pronounced elevation observed at 60 µg/mL. Moreover, enhanced activities of caspases-8, -9, and -3 confirmed the induction of apoptosis in glioblastoma cells. Collectively, these findings indicate that CsHw-EtOH effectively promotes apoptotic cell death, highlighting its therapeutic potential against GBM.

Keywords: Apoptosis, *Caesalpinia sappan*, Caspases, Glioblastoma multiforme, Reactive oxygen species

DOI: *https://doi.org/10.55734/nbujps.2025.v17i01.004*

Article info

Received **27 December 2025**
Revised **11 March 2026**
Accepted **17 March 2026**

Introduction

In humans, glioblastoma multiforme, abbreviated as GBM, is undoubtedly the most perilous form of brain tumors that originates either *de novo* or arises from a pre-existing astrocytoma. GBMs are characterized as highly malignant, proliferating, and mitotic tumors and hence are categorized as Grade IV tumors as per the classification of the World Health Organization (Marquet et al. 2007). GBM accounts for 60% of the total reported brain tumors and is categorized as primary and secondary glioblastoma (Tiwari et al. 2021a). Therapeutic approaches for GBM patients pose significant challenges due to heightened heterogeneity at both inter- and intra-tumoral levels, compounded by selective permeability, which in turn contributes to delayed early diagnosis. (Hanif et al. 2017). The disease becomes evident through the emergence of focal neural deficits, recurring headaches, seizures, and cognitive impairments. Undoubtedly, the primary treatment modality for GBM is precise surgical resection of the tumour. Nevertheless,

Correspondence: shahanamajumder@mgcub.ac.in

owing to the current challenges in achieving precise surgical removal and the invasive nature of these tumours, GBM patients who undergo surgery in conjunction with temozolomide typically experience a median survival time of just 12–15 months (Cantrell et al. 2019).

Being an important transcription factor, NF-κB is associated with the expression of key genes regulating various homeostatic functions, including cellular differentiation, proliferation, and survival within human cells. Unregulated NF-κB expression is a common phenomenon during the pathogenesis of multiple carcinomas, including GBM (Deka and Li 2023). The hyperactivation of NF-κB is mediated by various stimuli in GBM clinically. Altered NF-κB expression modulates stemness, invasiveness, and the development of chemotherapeutic resistance in GBM patients (Shi et al. 2023). Indeed, the role of NF-κB has previously been exhaustively studied in several cancers; nevertheless, its mechanistic role in GBM is yet to be elucidated completely.

Caesalpinia sappan L., commonly referred to as sappan wood, is a member of the *Fabaceae* family. The plant is abundant in various regions, including Southeast Asia, the southern provinces of China, and India, where it can be found either as a cultivated crop or in its wild form (Li et al. 2020). The plant is typically described as a shrubby tree that can reach a height of 10 meters, featuring alternate bipinnate leaves. It bears clusters of flat, oblong pods that contain brown, flattened, and ellipsoid seeds. The heartwood of this plant is dense and exhibits an orange-red hue. A rich source of numerous bioactive compounds is present in the *Caesalpinia* heartwood (CsHw), with homo-isoflavonoids being particularly prevalent. Among these compounds, brazilin, a natural red dye, stands out as the primary active ingredient in comparison to its oxidized counterpart, brazilein (Settharaksa et al. 2019; Uddin et al. 2015). The remarkable anti-cancer potential of Brazilin has also been widely reported, notably in various cancer cells, viz. MCF7, A549, HT29, HL60, U87, and K562 as reported in a recent publication (Jia et al. 2016; Islam et al. 2016).

Other important phytoconstituents of *C. sappan* include phenolic compounds, namely sappanol and episappanol, along with catechols, including protosappanin (Uddin et al. 2015, Islam et al. 2016). In the realm of traditional medicine, the heartwood of this plant has found diverse applications, including harnessing its potential for anti-inflammatory, anti-thrombotic, and neuroprotective effects, which are ascribed to the abundance of bioactive compounds it contains. Additionally, it has been used as a post-partum tonic to alleviate uterine bleeding. This plant also demonstrates its therapeutic potential for diarrhoea and sleep disorders (Zeng et al. 2015; Islam et al. 2016; Syamsunarno et al. 2021).

In the present study, the investigators focused on identifying the bioactive constituents of ethanolic extract of *Caesalpenia sappan* heartwood (CsHw-EtOH). Subsequently, the effect of CsHw-EtOH on the growth and apoptosis within rat glioblastoma C6 cells was also investigated. The observations explicitly indicated that CsHw-EtOH ameliorated the survival of C6 cells by instigating apoptotic cell death. Apoptotic cell death post-CsHw-EtOH was further found to be correlated with deflated NF-κB levels *in vitro*. Thus, it was inferred from this study that CsHw-EtOH exhibits therapeutic potential and can be developed as an alternative amleorative agent for GBM.

Materials and methods

Materials

Reagents for cell culture, including DMEM media, antibiotic-antimycotic mixture, fetal bovine serum (FBS), MTT dye, and DCFH-DA, were procured from HiMedia, Maharashtra, India. The caspases-8, -9, and -3 kit for colorimetric assay was procured from Abcam, Cambridge.

Methods

Cell culture

Rat glioblastoma C6 and murine alveolar macrophages J774A.1 cells were obtained commercially from the cell repository of the National Centre for Cell Sciences, India. Both these cells were allowed to proliferate in DMEM-high-glucose media containing fetal bovine serum (FBS; 5% v/v) and antibiotic-antimycotic solution (1% v/v). The cells were incubated in a controlled atmosphere constituted by 5% CO_2 at 37°C. Phase-contrast and fluorescence microscopy were conducted using the FLoid imaging station, Thermo-Scientific, USA, during this study.

Plant sample collection and authentication

The heartwood of *Caesalpinia sappan* was collected from Kayamkulam, Kerala, by Prof. Shahana Majumder, Department of Botany, MGCUB. The plant material was authenticated by the Jawaharlal Nehru Tropical Botanic Garden and Research Institute (JNTBGRI), Kerala, and assigned the accession number 5531 (TBGT).

Sample preparation

The air-dried heartwood of *C. sappan* was crushed using a grinder, and the resultant powder was properly packed in a Soxhlet apparatus for the preparation of ethanolic extract. The obtained solution was filtered using a Whatman paper filter and was allowed to dry using a Telstar Cryodos freeze-drier. The extract was then stored at 4°C in a sterile Eppendorf tube for subsequent analysis.

Identification of bioactive compounds

Various bioactive compounds present within CsHw-EtOH were identified through gas chromatography-mass spectrometry (GC-MS) as previously described (Alshehri et al. 2022). 2 µL of CsHw-EtOH was used during the analysis with a total running time of 54 min. The constituents of the extract were expressed as percentages, with peak areas normalized. Various constituents of CsHw-EtOH were identified by comparing the retention time indices along with mass spectra patterns with the National Institute of Standards and Technology (NIST) database.

Cytotoxicity evaluation of CsHw-EtOH

Ethanolic extract of *C. sappan* heartwood (CsHw-EtOH) was assessed for its cytotoxic potential against C6 cells through an MTT assay as previously stated (Tiwari et al. 2021a). Approximately 5×10^3 C6 cells/well were treated with 20, 40, and 60 µg/mL of CsHw-EtOH in a 96-well plate and were left undisturbed for 24 h in optimum tissue culture conditions. Subsequently, 10 µL of MTT dye (5 mg/mL) was supplemented in each treatment group, followed by an incubation of 4 h at 37°C. 100 µL of tissue culture-grade DMSO was further added to each well to solubilize the formazan crystals formed (if any). Finally, the absorbance of each well was recorded using a microplate reader (Bio-Rad, USA). The cytotoxic effects were interpreted in terms of the cell viability percentage of C6 cells using the formula

Morphological assessment after CsHw-EtOH treatment

Morphological characteristics of C6 cells after treatment with CsHw-EtOH were qualitatively assessed using phase-contrast microscopy as previously described (Tiwari et al. 2022). Initially, 1×10^4 C6 cells were treated with the above-stated concentrations of CsHw-EtOH for 24 h. Subsequently, the wells were visualized, and photomicrographs were recorded. Differences in the morphological characteristics were confirmed by comparing the overall morphology of C6 cells belonging to various treatment groups with that of the untreated control.

Effects of CsHw-EtOH exposure on ROS in C6 cells

The efficiency of CsHw-EtOH in instigating levels of intracellular ROS was examined through DCFH-DA staining as previously reported (Shekh et al. 2022). Approximately 1×10^4 C6 cells were exposed to 20, 40, and 60 µg/ml of CsHw-EtOH in a 96-well plate and were left undisturbed for 6 – 8 h. Thereafter, both treated and control C6 cells were treated with DCFH-DA (20 µM) followed by a short incubation of 30 min at room temperature. Subsequently, the cells were washed once using PBS (1X) and were monitored for changes in the DCFH-DA-mediated intensity of green fluorescence at excitation: emission: 482/18 nm: 532/59 nm.

CsHw-EtOH effects on caspase-8, -9, and -3 level

Alterations in the levels of caspase-8, -9, and -3 in glioblastoma C6 cells were assessed colorimetrically as per the process reported earlier (Khafagy et al. 2022). Briefly, the C6 cells post-CsHw-EtOH exposure for 24 h were seeded at a density of 3×10^6 cells/group, including an untreated control, in a 96-well plate. The cells were lysed and centrifuged for 1 min (10,000×*g* at 4°C). 50 µl of the supernatant was placed on ice and supplemented with an equal volume of reaction buffer constituted by 10 mM DDT. 4 mM of caspase-3, -8, -9 substrate, namely DEVD-pNA, IETD-pNA, and LEJD-pNA, respectively, were added in each group and incubated additionally for 10 min. Eventually, the absorbance of CsHw-EtOH-treated and/or untreated C6 cells was recorded at 405 nm. Results were expressed as caspase activity percentage relative to untreated control C6 cells.

Investigation of NF-κB/p65 release

The competency of CsHw-EtOH in reducing the inflammatory marker, such as NF-κB, was assessed colorimetrically. Expression levels of NF-κB/p65 were quantified in CsHw-EtOH-treated and/or untreated control C6 cells through ELISA (Abcam, Cambridge, UK) following the manufacturer's protocol.

Statistical inferences

The data reported in the study represent the mean ± SEM of triplicate experiments performed thrice individually. Statistical inferences were drawn after using one-way ANOVA followed by Dunnett post-hoc test. Mean differences between different groups were considered to be statistically significant when

$p<0.05$. The level of significance was represented as $*p<0.05$; $**p<0.01$, and $***p<0.001$.

Results

GC-MS Analysis-based identification of CsHw-EtOH bioactive compounds

The phytochemical compounds in CsHw-EtOH were analyzed by GC–MS analysis (Figure 1). The mass analysis revealed the presence of 45 compounds, as shown in Table 1. Previously, *C. sappan* has been reported to possess xanthone, coumarin, chalcones, flavones, homo-isoflavonoids, and brazilin (Vij et al. 2023). Intriguingly, during the present investigation, CsHw-EtOH revealed the presence of various phytoconstituents such as hydrocarbons, phenols, lactones, esters, aldehydes, sterols, and triterpenoids.

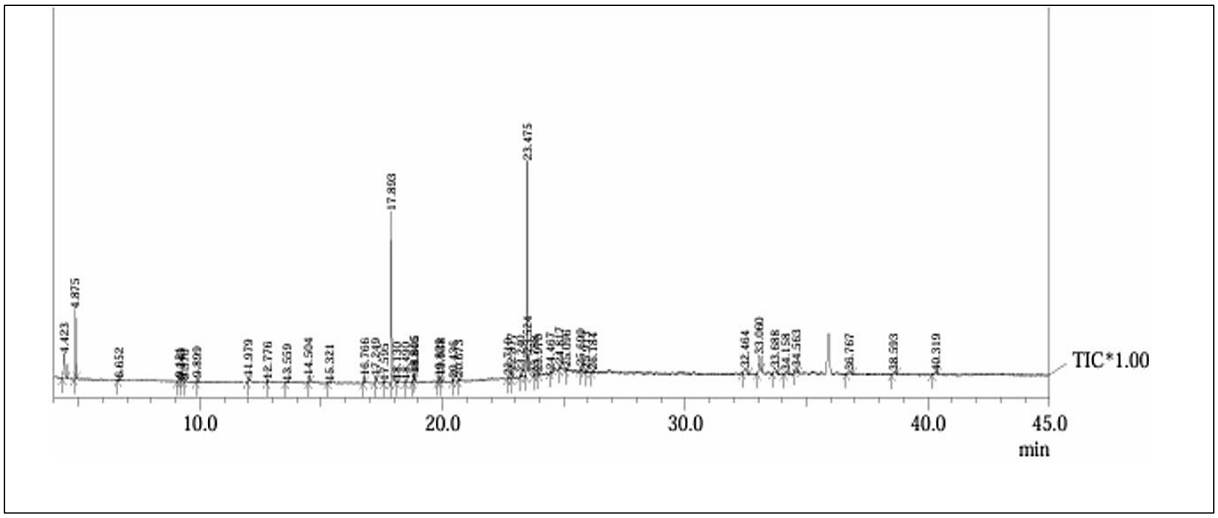

Figure 1. GCMS chromatogram of *C. sappan* heartwood ethanolic extract (CsHw-EtOH)

Table 1. List of various compounds identified through GC-MS analysis from CsHw-EtOH

S. No.	Peak Area	Area (%)	Identified compound	Molecular formula
1.	4.423	6.96	Cyclooctatetraene	C_8H_8
2.	4.875	9.61	2-Ethoxy-2-methylpropane	$C_6H_{14}O$
3.	6.652	0.12	1-Propenylaziridine	C_5H_9N
4.	9.121	0.68	1,1-dioctyloxyoctane	$C_{24}H_{50}O_2$
5.	9.240	0.18	2-Bromoooctane	$C_8H_{17}Br$
6.	9.370	0.11	(1R,3S)-7,7-dimethyl-2-oxabicyclo [4.1.1.] octan-3-one	$C_9H_{14}O_2$
7.	9.899	0.63	Isopropylcyclohexane	C_9H_{18}
8.	11.979	0.93	n-Octyl chloroformate	$C_9H_{17}ClO_2$
9.	12.776	0.39	(E, Z)-2-methyl-2-butenoic acid 3-hexenyl ester	$C_{11}H_{18}O_2$
10.	13.559	0.15	2-tert-Butyl-4-(1,1,3,3-tetramethylbutyl) phenol	$C_{18}H_{30}O$
11.	14.504	1.10	2-Tridecene, 1,1,1,2-tetrafluoro-, (Z)-	$C_{13}H_{22}ClF_3$
12.	15.321	0.12	3,6-2H (2] -(3RS,4RS,5RS,6RS)-3,4:5,6-diepoxycyclohex-1-ene	$C_6H_4D_2O_2$
13.	16.766	0.92	1-Octadecene	$C_{18}H_{36}$
14.	17.249	0.84	4-ethyl-4-hydroxybutanoic acid lactone	$C_6H_{10}O_2$
15.	17.595	0.13	3-hexenoic acid, 3-methyl-, methyl ester	$C_8H_{14}O_2$
16.	17.893	25.03	2-(diethylamino)-N-(2,6-dimethylphenyl) acetamide hydrochloride	$C_{14}H_{23}ClN_2O$
17.	18.130	0.34	Tetradecanoic acid, 12-methyl-, methyl ester	$C_{16}H_{32}O_2$
18.	18.490	0.23	2-methyl-6-beta-dribofuranosylimidazo [1,2-c] pyrimidin 5(6H)-one	$C_{12}H_{15}N_3O_5$
19.	18.805	0.81	Eicosanoic acid, ethyl ester	$C_{22}H_{44}O_2$

20.	18.841	0.35	Chrysene, 4b,5,6,12-tetrahydro-2,8-dimethoxy-4b-methyl-	$C_{21}H_{22}O_2$
21.	19.829	0.58	9-Octadecenoic acid (Z)-, methyl ester	$C_{19}H_{36}O_2$
22.	19.938	0.88	2-Isopropyl-5-methylcycloh exanol	$C_{10}H_{20}O$
23.	20.436	0.22	1-(Cyclohexylmethyl)-3-methylcyclohexane	$C_{14}H_{26}$
24.	20.673	0.48	6-Methyl-1-octanol	$C_9H_{20}O$
25.	22.710	0.39	16-Heptadecenal	$C_{17}H_{32}O$
26.	22.877	1.04	Benzfetamine	$C_{17}H_{21}N$
27.	23.240	0.53	3-Ethyl-5-(2'-ethylbutyl) octadecane	$C_{26}H_{54}$
28.	23.475	25.27	Benzyldiethyl-(2,6-xylylcarbamoylmethyl)-ammonium benzoate	$C_{28}H_{34}N_2O_3$
29.	23.524	0.69	Diisooctyl phthalate	$C_{24}H_{38}O_4$
30.	23.788	0.19	(2E,7E)-4,8,12-Trimethyl-2,7,11-tridecatrien-4-ol	$C_{16}H_{28}O$
31.	23.970	0.27	Ethyl tridecanoate	$C_{15}H_{30}O_2$
32.	24.467	0.42	β-D-Mannofuranoside, farnesyl-	$C_{21}H_{36}O_6$
33.	24.817	0.61	Oxalic acid, 6-ethyloct-3-yl heptyl ester	$C_{19}H_{36}O_4$
34.	25.096	0.48	Methyl 11-(2,3-dideuterocyclopentan-1-yl) undecanoate	$C_{17}H_{30}D_2O_2$
35.	25.699	0.67	Dodecanoic acid, ethyl ester	$C_{14}H_{28}O_2$
36.	25.913	0.26	Farnesyl acetate	$C_{17}H_{28}O_2$
37.	26.184	0.33	2-heptadec-5"-en-1"-yloxy tetrahydrofuran	$C_{22}H_{42}O_2$
38.	32.464	2.65	1-Heptatriacotanol	$C_{37}H_{76}O$
39.	33.060	5.52	Stigmasterol	$C_{29}H_{48}O$
40.	33.688	2.10	Lanosterol	$C_{30}H_{50}O$
41.	34.158	1.15	Methanol, [5,7,9-trimethyl-4-(1-propenyl)-3-oxabicyclo [3.3.1] non-6-en-1-yl]	$C_{15}H_{24}O_2$
42.	34.563	1.52	S-[2-(3,22,26-Trihydroxycholestan-16-yl) ethyl] thioformate	$C_{30}H_{52}O_4S$
43.	36.767	1.60	Methanol, [5,7,9-trimethyl-4-(1-propenyl)-3-oxabicyclo [3.3.1] non-6-en-1-yl]-	$C_{15}H_{24}O_2$
44.	38.593	1.37	1,4-dimethyl-3-(2-methyl-1-propenyl)-4-vinyl-1-cycloheptene	$C_{15}H_{24}$
45.	40.319	1.10	(3,3-Dimethyl-2-[(1E)-3-methyl-1,3-butadienyl] cyclohexyl) methanol	$C_{14}H_{24}O$

CsHw-EtOH exerted cytotoxic effects against C6 cells

The cytotoxic potential of CsHw-EtOH against glioblastoma C6 cells was evaluated at different concentrations of 20, 40, and 60 µg/mL. The findings during the cytotoxicity estimation revealed that CsHw-EtOH reduced the cell viability of C6 cells. The viability of C6 cells post-CsHw-EtOH exposure was reduced to 89.59 ± 4.14 (20 µg/mL), 79.47 ± 4.66 (40 µg/mL), and 39.85 ± 3.71 (60 µg/mL). The reduction in the viable number of C6 compared to untreated control cells indicated the cytotoxic attributes of CsHw-EtOH against C6 cells (Figure 2A). The IC50 of CsHw-EtOH was further calculated using the stated concentrations and was found to be 25.34 ± 1.34 µg/mL (Figure 2B). Intriguingly, CsHw-EtOH failed to induce any substantial cytotoxic effects against murine alveolar macrophage J774A.1 cells.

Exposure to CsHw-EtOH altered C6 cellular morphology

The effect of CsHw-EtOH in altering C6 cellular morphology was also assessed to further validate its toxic effect. Bright-field microscopic evaluation of CsHw-EtOH-treated C6 cells clearly indicated enhanced plasma membrane bulging, cell rupturing, and reduced confluency. These attributes more or less indicated a plausible onset of apoptotic pathways within C6 cells. Indeed, the number of floating dead cells increased proportionally with an increase in CsHw-EtOH concentration (Figure 2C).

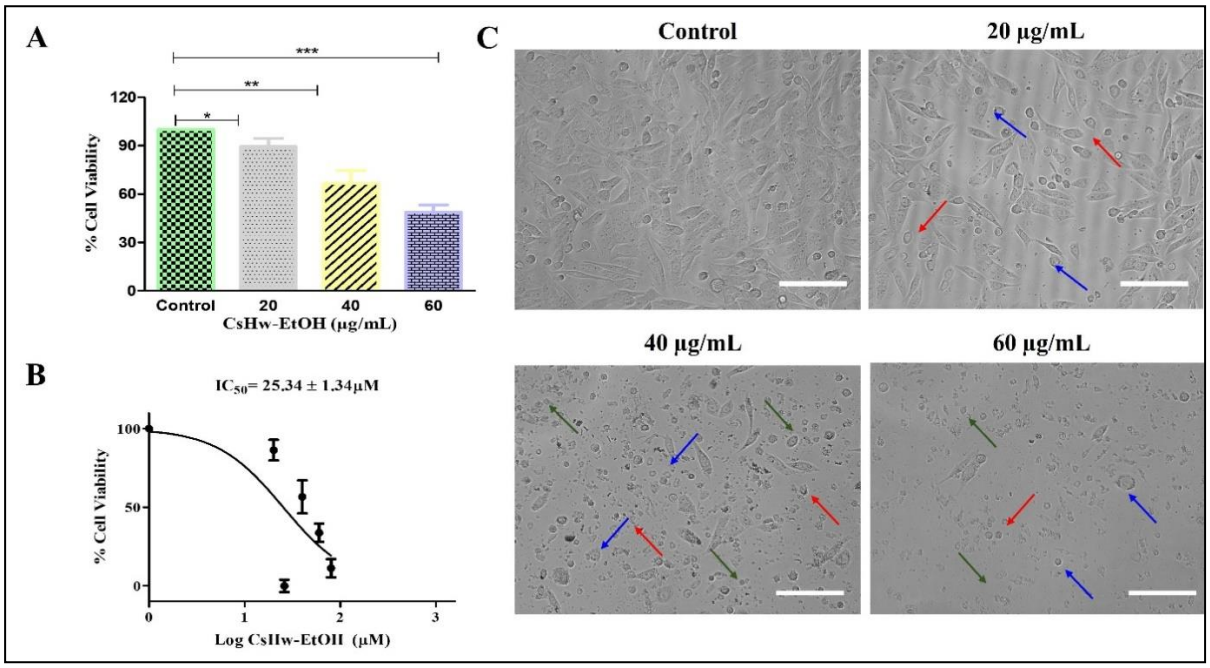

Figure 2. Cytotoxic effects of CsHw-EtOH against Glioblastoma C6 cells as interpolated through (A) Cell viability percentage post-CsHw-EtOH treatment after 24 h at 20-60 µg/mL concentration, (B) The IC50 value of CsHw-EtOH, and (C) changes in the morphology of CsHw-EtOH-treated C6 cells. Red arrows indicate rounding of cells, blue arrows indicate blebbing of the plasma membrane, and green arrows indicate disintegration of cell organelles. Magnification = 20X, Scale bar =100 µm. *p<0.05; **p<0.01 and ***p<0.001.

CsHw-EtOH induced oxidative stress in C6 cells

ROS-mediated escalation in oxidative stress is a crucial instigator of apoptotic pathways in a caspase-dependent and/or caspase-independent pathway. Therefore, to explore the CsHw-EtOH-induced cytotoxicity mechanism, the ROS-mediated level of oxidative stress was further investigated. The C6 cells exposed to varying CsHw-EtOH concentrations demonstrated a dose-dependent increase in the characteristic DCF-DA-induced green fluorescence. Higher intensity of DCF-DA stain clearly indicated an elevated level of ROS production in glioblastoma C6 cells.

Subsequently, the levels of intracellular ROS were quantified through DCF-DA-induced average fluorescence intensity percentage (DCF-DA MFI%). The DCF-DA MFI% was found to be 22.71 ± 3.79% and 37.01 ± 3.27% at 20 µg/mL and 40 µg/mL, respectively, which further augmented to 62.75 ± 4.06% at 60 µg/mL (Figure 3).

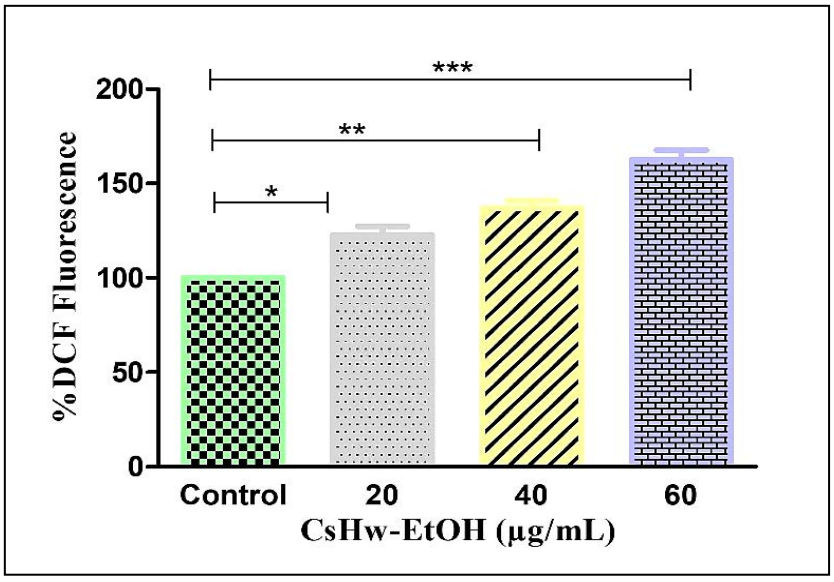

Figure 3. Efficacy of CsHw-EtOH in inducing intracellular ROS, as determined by quantitative analysis of DCF-DA–mediated fluorescence intensity. *p<0.05; **p<0.01 and ***p<0.001.

CsHw-EtOH exposure activated caspases in C6 cells

The efficacy of CsHw-EtOH in activating key caspases within rat glioblastoma C6 cells was further explored. Observation showed that CsHw-EtOH exposure triggered the activation of caspase-3 following a dose-dependent trend. Concomitantly, the levels of caspase-8 and caspase-9 activity were also found to be significantly elevated upon exposure of C6 cells to CsHw-EtOH. Intriguingly, the activity of caspase-8 and -9 was found to be significant at higher CsHw-EtOH concentrations of 40 and 60 µg/ml (Figure 4).

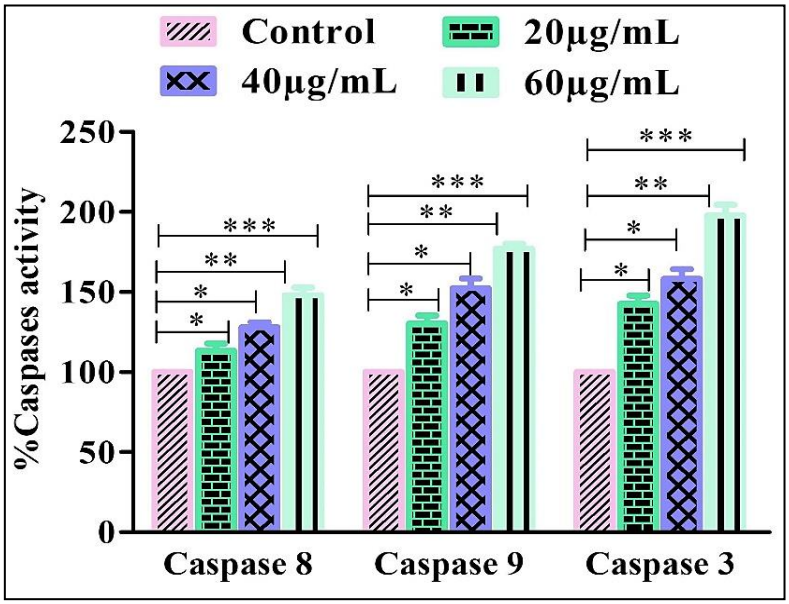

Figure 4. Efficacy of CsHw-EtOH in activating caspase-8, -9, and -3 in C6 cells post-treatment with 20, 40, and 60 µg/mL of CsHw-EtOH. *p<0.05; **p<0.01 and ***p<0.001.

CsHw-EtOH mediates inhibition of NF-κB and its associated genes

Aberrant activation of NF-κB is frequently reported in various malignancies, including GBM. Consequently, to investigate the underlying anticancer and apoptotic mechanism of CsHw-EtOH in C6 cells, the levels of NF-κB/p65 were estimated using Enzyme-Linked Immunosorbent Assay (ELISA). The results demonstrated that CsHw-EtOH decreased the levels of NF-κB/p65 to 3.67 ± 1.14 ng/mL, as compared to the untreated cells (Figure 5).

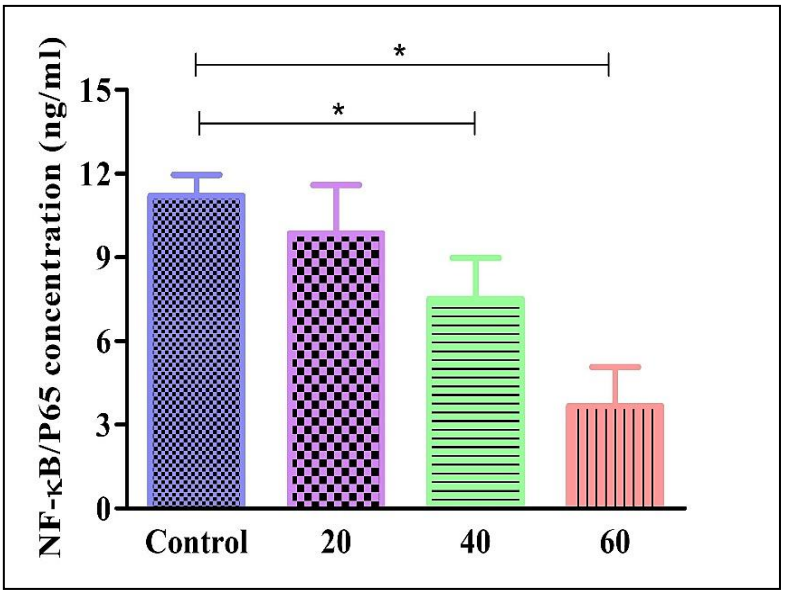

Figure 5. The efficacy of CsHw-EtOH in deflating the levels of NF-κB in C6 cells treated at 20- 60 µg/mL concentration. *p<0.05; **p<0.01 and ***p<0.001.

Discussion

Investigations focusing on the search for novel therapeutic interventions against different forms of cancer have escalated globally (Carneiro and El-Deiry, 2020). Indeed, the apoptosis-inducing efficacy of any therapeutic is regarded as an effective interventional strategy against several cancers (Lim et al. 2019). At present, natural compounds are being explored globally as potential novel chemotherapeutics since the majority of chemotherapeutics used today, including vincristine, paclitaxel, and docetaxel, have all been derived from natural products (Cragg and Newmann, 2005).

Caesalpinia sappan L. is a representative of the *Leguminosae* family and is also commonly referred to as Sappan or Brazil wood. *C. sappan* is distributed geographically throughout the Southeast Asian region, and its heartwood has been traditionally used in food and beverages (Toegel et al. 2012). Indeed, *C. sappan* heartwood (CsHw) has been a source of purified red dye. Intriguingly, *C. sappan* heartwood has been an important source for treating skin infections, tuberculosis, dysentery, and anaemia (Sireeratawong et al. 2010). Chemical investigations of CsHw have shown the presence of various bioactive compounds, namely coumarin, xanthone, flavones, and flavonoids. Moreover, brazilin has been identified as a major naturally occurring bioactive compound in CsHw, which is subsequently used as a red stain during microanatomic studies (Bae et al. 2005). CsHw has also been used in Indian Ayurvedic and traditional Chinese folk medicine for its anti-inflammatory, pro-analgesic, enhancing blood circulation, and menstruation promoting properties (Nirmal et al. 2015).

In this study, 45 compounds have been detected in the ethanolic extract from the heartwood of *C. sappan* by GC–MS analysis. The GC–MS chromatogram indicated the presence of different bioactive phytoconstituents such as hydrocarbons, phenols, lactones, esters, aldehydes, sterols, and triterpenoids, which could be responsible for their anticancer efficacy. Stigmasterol and lanosterol were one of the major compounds, representing peak areas of 5.52% and 2.10%, respectively. Stigmasterol possesses various potent pharmacological properties such as anticancer, anti-osteoarthritis, anti-inflammatory, anti-diabetic, immunomodulatory, antiparasitic, antifungal, antibacterial, antioxidant, and neuroprotective properties (Bakrim et al. 2022). Oxalic acid, 6-ethyloct-3-yl heptyl ester, as one of the major constituents of *Breynia cernua* stem extract, exhibited anti-inflammatory, antibacterial, antioxidant, anthelmintic, antidiabetic, anticancer, mosquitocidal, and insecticidal activity (Wiraswati et al. 2023). Intriguingly, in the recent past, studies have elucidated the anticancer potential of CsHw against cancers such as breast cancer (MCF7) and lung cancer (A549) and cervical cancer HeLa cells (Hung et al. 2014; Widodo et al. 2022). Nevertheless, the anti-cancer efficacy of CsHw-EtOH against glioblastoma multiforme remains elusive. Pertaining to this elusiveness, the investigators tried to explore the anti-cancer effects of CsHw-EtOH against murine glioblastoma C6 cells.

In the present report, it was observed that CsHw-EtOH impeded the growth of C6 cells. During the MTT assay, CsHw-EtOH significantly reduced the viability of C6 cells. Thus, it was concluded that CsHw-EtOH inhibited the growth of C6 cells, which indicated the probable cytotoxic effects of CsHw-EtOH against C6 cells. However, CsHw-EtOH failed to exert similar cytotoxic effects against normal murine alveolar macrophage J774A.1 cells. This observation was further affirmed by the photomicrographs depicting the alterations in morphological features of CsHw-EtOH-treated C6 cells. Indeed, the exposure of CsHw-EtOH instigated characteristic changes in the morphology of C6 cells, which in turn are closely related to cell death.

Enhanced oxidative stress resulting from elevated ROS levels has been strongly associated with irreparable DNA damage, ultimately triggering apoptotic cell death (Yang et al. 2017). ROS-mediated DNA damage is a well-recognized initiator of apoptosis (Su et al. 2013; Zorov et al. 2014). In the present study, CsHw-EtOH treatment markedly increased intracellular ROS production, which may have initiated a cascade of events leading to C6 glioblastoma cell death. Mitochondria are recognized as the primary source of sterile ROS generation, and excessive mitochondrial ROS accumulation leads to dissipation of the mitochondrial membrane potential ($\Delta\Psi m$) and opening of mitochondrial permeability transition pores (Zorov et al. 2014). This process facilitates the release of cytochrome-c into the cytosol, thereby promoting apoptotic signaling (Zhang et al. 2015). Furthermore, compromised mitochondrial integrity is closely associated with the activation of caspase-3, a key executioner of apoptosis (Zhu et al. 2012). Consistent with these mechanisms, our findings demonstrate that CsHw-EtOH impaired mitochondrial viability in C6 cells, resulting in the activation of caspases-3, -8, and -9. These results indicate that CsHw-EtOH induces apoptotic cell

death through the activation of both intrinsic and extrinsic apoptotic pathways.

Aberrant activation of the NF-κB signaling pathway, known for its anti-apoptotic role, has been frequently reported in glioblastoma multiforme (GBM). Notably, overexpression of the NF-κB p65 subunit has been documented in gliomas (Raychaudhuri et al. 2007). Crosstalk between the NF-κB and p53 pathways has been shown to regulate cell cycle arrest and apoptosis in GBM (Cahill et al. 2016). In the present investigation, CsHw-EtOH treatment significantly downregulated NF-κB/p65 expression in C6 cells, suggesting effective inhibition of NF-κB signaling. This suppression likely contributed to the modulation of downstream target genes involved in cellular proliferation and apoptotic resistance, thereby enhancing apoptosis in glioblastoma cells.

Conclusion

In conclusion, our present report has demonstrated that CsHw-EtOH exerts anticancer efficacy by suppressing the growth and mediating programmed cell death in human GBM C6 cells by impeding the activation of NF-κB. These results indicate that the potential CsHw-EtOH should be further studied as an anti-GBM drug in various pre-clinical and clinical studies. However, subsequent in-depth studies are still required to explore the exact mechanism of apoptosis induced by CsHw-EtOH in GBM cells.

Conflict of Interest: The authors of this manuscript hold no potential conflict of interest among themselves.

Funding

Not Available.

References

Bae IK, Min HY, Han AR, Seo EK, Lee SK (2005) Suppression of lipopolysaccharide-induced expression of inducible nitric oxide synthase by brazilin in RAW 264.7 macrophage cells. *European Journal of Pharmacology* 513: 237–242. https://doi.org/10.1016/j.ejphar.2005.03.021

Cahill KE, Morshed RA, Yamini B (2015) Nuclear factor-κB in glioblastoma: insights into regulators and targeted therapy. *Neuro-Oncology* 18: 329–339. https://doi.org/10.1093/neuonc/nov268

Cantrell JN, Waddle MR, Rotman M, Peterson JL, Ruiz-Garcia H, Heckman MG, Trifiletti DM (2019) Progress toward long-term survivors of glioblastoma. *Mayo Clinic Proceedings* 94: 1278–1286. https://doi.org/10.1016/j.mayocp.2018.12.030

Carneiro BA, El-Deiry WS (2020) Targeting apoptosis in cancer therapy. *Nature Reviews Clinical Oncology* 17: 395–417. https://doi.org/10.1038/s41571-020-0341-y

Cragg GM, Newman DJ (2005) Plants as a source of anti-cancer agents. *Journal of Ethnopharmacology* 100: 72–79. https://doi.org/10.1016/j.jep.2005.05.011

Deka K, Li Y (2023) Transcriptional regulation during aberrant activation of NF-κB signalling in cancer. *Cells* 12: 788. https://doi.org/10.3390/cells12050788

Hanif F, Muzaffar K, Perveen K, Malhi SM, Simjee SU (2017) Glioblastoma multiforme: a review of its epidemiology and pathogenesis through clinical presentation and treatment. *Asian Pacific Journal of Cancer Prevention* 18: 3–9. https://doi.org/10.22034/APJCP.2017.18.1.3

Hung TM, Dang NH, Dat NT (2014) Methanol extract from Vietnamese *Caesalpinia sappan* induces apoptosis in HeLa cells. *Biological Research* 47: 20. https://doi.org/10.1186/0717-6287-47-20

Islam MA, Alam F, Ibrahim Khalil M, Haryo Sasongko T, Hua Gan S (2016) Natural products towards the discovery of potential future antithrombotic drugs. *Current Pharmaceutical Design* 22: 2926–2946. https://doi.org/10.2174/1381612822666160325145522

Jia Y, Zhao J, Liu M, Li B, Song Y, Li Y, Shi L (2016) Brazilin exerts protective effects against renal ischemia-reperfusion injury by inhibiting the NF-κB signaling pathway. *International Journal of Molecular Medicine* 38: 210–216. https://doi.org/10.3892/ijmm.2016.2615

Khafagy ES, Al Saqr A, Alotaibi HF, Abu Lila AS (2022) Cytotoxic and apoptotic effect of *Rubus chingii* leaf extract against non-small cell lung carcinoma A549 cells. *Processes* 10: 1537. https://doi.org/10.3390/pr10081537

Li LM, Fu JX, Song XQ (2020) Complete plastome sequence of *Caesalpinia sappan* Linnaeus, a dyestuff and medicinal species. *Mitochondrial DNA Part B* 5: 2535–2536. https://doi.org/10.1080/23802359.2020.1782578

Lim B, Greer Y, Lipkowitz S, Takebe N (2019) Novel apoptosis-inducing agents for the treatment of cancer, a new arsenal in the toolbox. *Cancers* 11: 1087. https://doi.org/10.3390/cancers11081087

Marquet G, Dameron O, Saikali S, Mosser J, Burgun A (2007) Grading glioma tumors using OWL-DL and NCI thesaurus. *AMIA Annual Symposium Proceedings* 2007: 508–512.

Nirmal NP, Rajput MS, Prasad RG, Ahmad M (2015) Brazilin from *Caesalpinia sappan* heartwood and its pharmacological activities: A review. *Asian Pacific Journal of Tropical Medicine* 8: 421–430. https://doi.org/10.1016/j.apjtm.2015.05.005

Raychaudhuri B, Han Y, Lu T, Vogelbaum MA (2007) Aberrant constitutive activation of nuclear factor κB in glioblastoma multiforme drives invasive phenotype. *Journal of Neuro-Oncology* 85: 39–47. https://doi.org/10.1007/s11060-007-9392-5

Settharaksa S, Monton C, Charoenchai L (2019) Optimization of *Caesalpinia sappan* L. heartwood extraction procedure to obtain the highest content of brazilin and greatest antibacterial activity. *Journal of Integrative Medicine* 17: 351–358. https://doi.org/10.1016/j.joim.2019.06.004

Shekh R, Tiwari RK, Ahmad A, Ahmad I, Alabdallah NM, Saeed M, Bajpai P (2022) Ethanolic extract of *Coleus aromaticus* leaves impedes the proliferation and instigates apoptotic cell death in liver cancer HepG2 cells through repressing JAK/STAT cascade. *Journal of Food Biochemistry* 46: e14368. https://doi.org/10.1111/jfbc.14368

Shi P, Xu J, Cui H (2023) The recent research progress of NF-κB signaling on the proliferation, migration, invasion, immune escape and drug resistance of glioblastoma. *International Journal of Molecular Sciences* 24: 10337. https://doi.org/10.3390/ijms241210337

Sireeratawong S, Piyabhan P, Singhalak T, Wongkrajang Y, Temsiririrkkul R, Punsrirat J, Jaijoy K (2011) Toxicity evaluation of sappan wood extract in rats. *Journal of the Medical Association of Thailand* 93: S50–S57.

Su J, Lai H, Chen J, Li L, Wong YS, Chen T, Li X (2013) Natural borneol, a monoterpenoid compound, potentiates selenocystine-induced apoptosis in human hepatocellular carcinoma cells by enhancement of cellular uptake and activation of ROS-mediated DNA damage. *PLoS ONE* 8: e63502. https://doi.org/10.1371/journal.pone.0063502

Syamsunarno MRA, Safitri R, Kamisah Y (2021) Protective effects of *Caesalpinia sappan* Linn. and its bioactive compounds on cardiovascular organs. *Frontiers in Pharmacology* 12: 725745. https://doi.org/10.3389/fphar.2021.725745

Tiwari RK, Ahmad A, Khan MS, Shahanawaz SD, Ahmad S, Ansari IA (2022) Pinostrobin suppresses the proliferation of lung carcinoma cells by abrogating the cell cycle progression through the inhibition of Notch signaling pathway. *South African Journal of Botany* 151: 614–622. https://doi.org/10.1016/j.sajb.2022.09.010

Tiwari RK, Singh S, Gupta CL, Bajpai P (2021a) Microglial TLR9: plausible novel target for therapeutic regime against glioblastoma multiforme. *Cellular and Molecular Neurobiology* 41: 1391–1393. https://doi.org/10.1007/s10571-020-00935-0

Toegel S, Wu SQ, Otero M, Goldring MB, Leelapornpisid P, Chiari C, Viernstein H (2012) *Caesalpinia sappan* extract inhibits IL1β-mediated overexpression of matrix metalloproteinases in human chondrocytes. *Genes & Nutrition* 7: 307–318. https://doi.org/10.1007/s12263-011-0252-8

Uddin GM, Kim CY, Chung D, Kim KA, Jung SH (2015) One-step isolation of sappanol and brazilin from *Caesalpinia sappan* and their effects on oxidative stress-induced retinal death. *BMB Reports* 48: 289–294. https://doi.org/10.5483/BMBRep.2015.48.5.290

Widodo N, Puspitarini S, Widyananda MH, Alamsyah A, Wicaksono ST, Masruri M, Jatmiko YD (2022) Anticancer activity of *Caesalpinia sappan* by downregulating mitochondrial genes in A549 lung cancer cell line. *F1000Research* 11: 169. https://doi.org/10.12688/f1000research.109351.1

Yang J, Zhao X, Tang M, Li L, Lei Y, Cheng P, Yuan Z (2017) The role of ROS and subsequent DNA-damage response in PUMA-induced apoptosis of ovarian cancer cells. *Oncotarget* 8: 23492–23506. https://doi.org/10.18632/oncotarget.15547

Zeng KW, Liao LX, Zhao MB, Song FJ, Yu Q, Jiang Y, Tu PF (2015) Protosappanin B protects PC12 cells against oxygen–glucose deprivation-induced neuronal death by maintaining mitochondrial homeostasis via induction of ubiquitin-dependent p53 protein degradation. *European Journal of Pharmacology* 751: 13–23. https://doi.org/10.1016/j.ejphar.2015.01.037

Zhang Y, Zhang X, Huang J, Dong Q (2015) Wnt signaling regulation of stem-like properties in

human lung adenocarcinoma cell lines. *Medical Oncology* 32: 157. https://doi.org/10.1007/s12032-015-0613-3

Zhu Y, Li M, Wang X, Jin H, Liu S, Xu J, Chen Q (2012) Caspase cleavage of cytochrome c1 disrupts mitochondrial function and enhances cytochrome c release. *Cell Research* 22: 127–141. https://doi.org/10.1038/cr.2011.149

Zorov DB, Juhaszova M, Sollott SJ (2014) Mitochondrial reactive oxygen species (ROS) and ROS-induced ROS release. *Physiological Reviews* 94: 909–950. https://doi.org/10.1152/physrev.00026.2013

Alshehri A, Ahmad A, Tiwari RK, Ahmad I, Alkhathami AG, Alshahrani MY, Ansari IA (2022) In vitro evaluation of antioxidant, anticancer, and anti-inflammatory activities of ethanolic leaf extract of *Adenium obesum*. *Frontiers in Pharmacology* 13: 847534. https://doi.org/10.3389/fphar.2022.847534

Vij T, Anil PP, Shams R, Dash KK, Kalsi R, Pandey VK, Shaikh AM (2023) A comprehensive review on bioactive compounds found in *Caesalpinia sappan*. *Molecules* 28: 6247. https://doi.org/10.3390/molecules28176247

Bakrim S, Benkhaira N, Bourais I, Benali T, Lee LH, El Omari N, Bouyahya A (2022) Health benefits and pharmacological properties of stigmasterol. *Antioxidants* 11: 1912. https://doi.org/10.3390/antiox11101912

Wiraswati HL, Fauziah N, Pradini GW, Kurnia D, Kodir RA, Berbudi A, Ma'ruf IF (2023) *Breynia cernua*: chemical profiling of volatile compounds in the stem extract and its antioxidant, antibacterial, antiplasmodial and anticancer activity in vitro and in silico. *Metabolites* 13: 281. https://doi.org/10.3390/metabo13020281